Jia *et al.*
Journal of Engineering and Applied Science (2024) 71:14
https://doi.org/10.1186/s44147-023-00354-x

Journal of Engineering and Applied Science

RESEARCH Open Access

Structural optimization and performance improvement of rock drill seals based on orthogonal test

Chunqiang Jia[1*], Aofei Wang[1], Li Zong[1] and Ling Yu[2]

*Correspondence:
jiacq229@126.com

[1] School of Mechanical Engineering, Shenyang Jianzhu University, Shenyang, China
[2] School of Mechanical Engineering, Shenyang University of Chemical Technology, Shenyang, China

Abstract

The drill tail of a rock drill meets high-frequency fretting in both the rotational and axial axes. The pure water seal is prone to damage and failure owing to its difficult working features and the low viscosity of the water medium. Orthogonal testing is used to simulate and model the Y-shaped seal ring to enhance the performance of the water seal. The maximum contact stress and maximum Von Mises stress are selected as indicators of sealing effectiveness based on an assessment of the effects of different seal section parameters on sealing performance. These insights serve to improve the building of the water seal. Maximum contact stress is demonstrated to be linked to lip thickness and chamfer length, but inversely proportional to lip length. Meanwhile, the maximum Von Mises stress is directly influenced by lip depth, including the angle of the lip and drill tail, and is inversely linked to lip thickness. Maximum contact stress and maximum Von Mises stress are lowered by 15% and 45%, respectively, in the revised Y-shaped water seal, resulting in greatly better sealing performance.

Keywords: Finite element method, Y-shaped water seal, Orthogonal test, Sealing performance

Introduction

In rock drilling operations, hydraulic drills are often employed. However, owing to the peculiar features of rock drill motion, the Y-shaped seal ring positioned between the drill tail and the washing head is sensitive to high-frequency impact and rotating motion, and water lubrication may not give appropriate protection. This may result in seal failure. Scholars in China and across the globe have lately undertaken extensive studies on the structure of the Y-shaped seal ring. Lei [1] utilized ANSYS to analyze the performance of the seal ring when subjected to changes in seal lip heights during reciprocating motion. They identified a connection between lip height and contact stress. Wang [2] simulated and evaluated the Y-shaped sealing ring for the reciprocating shaft, obtaining stress distribution in both the inner and outer lips, as well as contact stress changes during inward and outward strokes. Li [3] developed a finite element model to examine the static seal ring of a newly designed flat gate valve on a Christmas tree. Their study looked at the influence of the quantity of serrations on the lip, as well as the presence

of angles on both the lip and the lip valley, on sealing performance. Liu [4] explored the essential design aspects of a Y-shaped seal ring. Using ANSYS, Liu [5] employed the orthogonal test approach to develop a two-dimensional axisymmetric geometric model of the X-shaped sealing ring for the reciprocating piston rod. The research studied the impact of factors, including groove structure, retainer ring structure, installation status, and operating circumstances, on sealing efficacy and dependability. Gao [6, 7] applied the orthogonal test technique to explore the structure of a revolving seal ring. The peak contact stress and line contact pressure were applied as metrics for measuring sealing performance. Furthermore, the influence of each structural component on the sealing performance was examined, and the optimal model size parameters were established. Mevlüt [8] researched the elements that affect the longevity of ultra-high-molecular-weight polyethylene and polytetrafluoroethylene seals in ultra-high-pressure systems. To boost the effectiveness of drilling sealing materials, silicon dioxide, sodium silicate, and styrene acrylic emulsion were used to optimize the pore structure [9]. Utilizing uniaxial compression tests, nuclear magnetic resonance imaging, scanning electron microscopy, and fractal analysis, the impacts of each material on the pore structure and physical strength of the sealing materials were studied qualitatively and quantitatively.

Current research largely focuses on water seal structures in rock drills working under purely rotary, reciprocating, or static sealing circumstances. However, minimal research exists on dynamic sealing structures under the combined effect of both rotary motion and impact. To overcome this gap, we performed finite element simulations to assess the sealing stress state under combined rotation and impact situations. We discovered the indicators influencing sealing performance and utilized the orthogonal test technique to optimize the structural characteristics of the Y-shaped water seal in the rock drill washing mechanism. This work serves as a theoretical reference for the optimized design and performance enhancement of rock drill seals.

Methods

In this study, the optimization design of the Y-ring is realized through a series of steps. Firstly, the geometric size of the Y-ring is determined. Secondly, the finite element model is established in Abaqus according to the actual size, and a series of key information such as material properties, grid properties, and boundary conditions are set up. In the visualization, the maximum contact stress and the maximum Von Mises stress are used as effective indicators of sealing performance. Finally, the influence law of each parameter of the Y-ring is studied by orthogonal experiment, and the Y-ring is further optimized and analyzed.

Geometric model

The rock drill's flushing mechanism contains a drill tail, a sleeve for water injection, and two Y-shaped seal rings (shown in Fig. 1). During its operation, the drill tail suffers impact owing to the rotating and reciprocating motions, which enable it to drill into rocks. The two Y-shaped seals are utilized to secure the high-pressure cleansing water within. Considering the combined impact and rotating actions on the rock drill and the low viscosity of pure water, it is difficult to build a stable dynamic-pressure lubricating layer. Hence, the water seal is prone to deterioration.

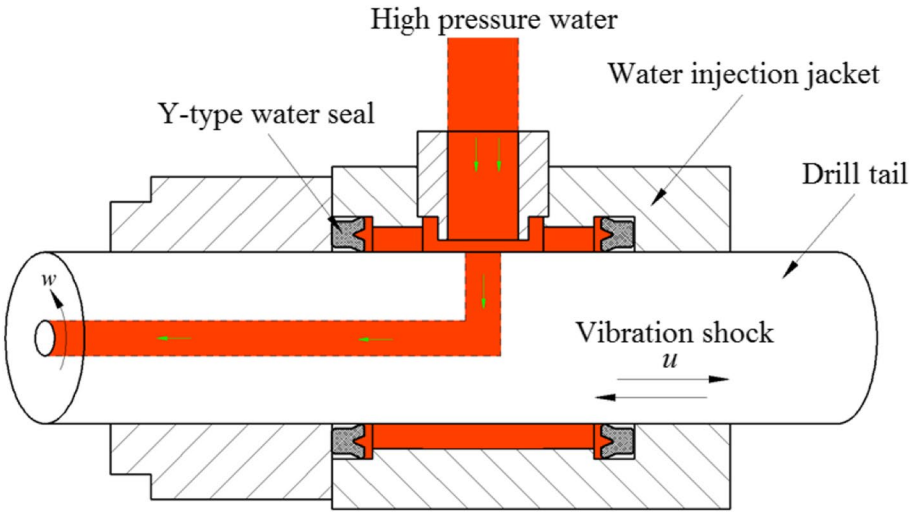

Fig. 1 Structure of flushing mechanism of rock drill

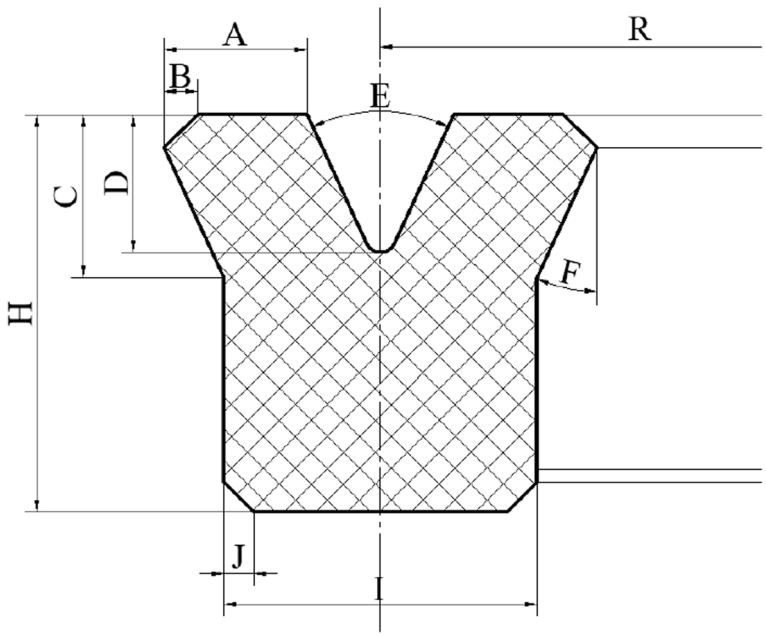

Fig. 2 Parametric model of Y-ring

This study focuses on the Y-shaped seal ring in the washing mechanism of a rock drill. The seal runs at a frequency of 50 Hz, spins at a speed of 350 r/min, and is exposed to a washing water pressure of 3 MPa. The Y-seal has dimensions of $Y40 \times 50 \times 6$ and is composed of hydrolysis-resistant polyurethane. Relevant dimensions include $A = 2$ mm, $B = 0.47$ mm, $C = 2.3$ mm, $D = 1.9\,5$ mm, $E = 50°$, and $F = 25°$, as shown in Fig. 2.

Finite element simulation model

Simulation model establishment

A simplified simulation model was developed taking into account the number of test groups in the orthogonal test method in order to increase computational efficiency. A 0.2-mm cross-section of the seal ring that has been unfolded onto a plane to line up with the drill tail is shown in Fig. 3. The movement of the Y-shaped seal ring along the X and Y axes simulate the rotary and impact actions of the rock drill's washing system.

The widely utilized Mooney-Rivlin constitutive model is employed to represent the mechanical behavior of polyurethane materials in engineering applications. The drill tail and water injection jacket are composed of structural steel with an elastic modulus of 210,000 MPa, a Poisson's ratio of 0.3, and a density of 7.85×10^{-9} t/mm^3. Polyurethane is used to create Y-shaped seals. Relevant assumptions are made in order to model nonlinear material properties [10, 11]. The Lagrange method is applied to the compact problem during simulation, with a friction coefficient of 0.3. To enhance the precision of the simulation of the rock drill's Y-type water seal, the properties of the three components of the simulation model—the braze tail and the Y-type water seal—are defined using the hexahedral C3D8R cell with linear reduced integration. These components are susceptible to mesh twisting and deformation caused by rotational impact. The swept mesh of the water injection sleeve and the Y-type water seal is divided by the progression algorithm, while the swept mesh of the braze tail is divided by the neutral axis algorithm and the minimum mesh transition is utilized to enhance the mesh quality. These divisions are made when defining the mesh attributes of the three components of the simulation model. There are 10,789 nodes and 6729 units in the entire model.

When the global size is 0.5, the total number of Y-seal nodes is 7470, the total number of cells is 4784, and the maximum Von Mises stress is 7.5 MPa. When the global size is 0.4, the maximum Von Mises stress is 7.512 MPa, and when the global size is 0.2, the maximum Von Mises stress is 7.52 MPa. The error range is very small, and it verifies the independence of the grid.

The finite element analysis procedure is broken down into three steps based on the Y-shaped seal ring's sealing principle and the drill's washing mechanism structure. Step 1: preload the Y-shaped sealing ring to 0.8 mm by applying a radial displacement to the water injection sleeve; Step 2: apply 3 MPa of water pressure to the sealing ring to

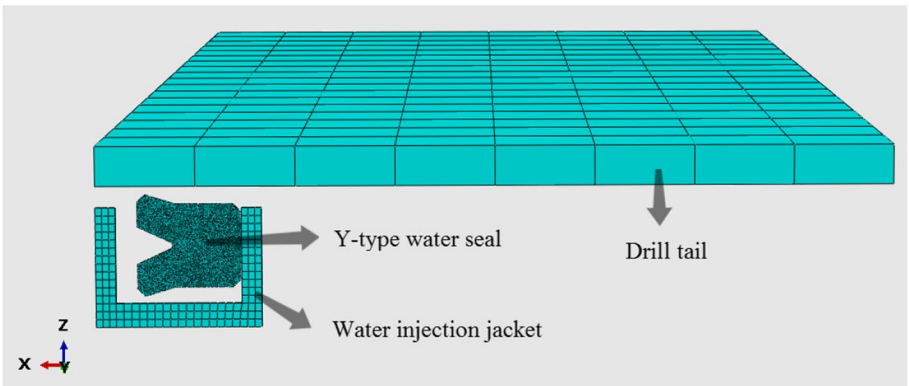

Fig. 3 Finite element analysis model

guarantee a high-pressure water seal state; Step 3: permit the fiber tail to move in both X and Y directions to replicate the rotary and impact movement of the rock drill's washing mechanism.

Simulation model verification

We used experimental data from pertinent literature and set the same parameters in the simulation model to confirm its efficacy [12]. The target parameter for comparison and validation was determined to be the seal ring's friction.

As illustrated in Fig. 4, there is a high degree of agreement between the simulated and experimental results regarding the trend of seal ring friction variation with speed. There is a minimal discrepancy between the two data sets. The difference is within 10%, indicating the credibility of the simulation outcomes.

Extracting sealing performance indicators from simulation

Von Mises stress and contact stress maps were produced for the Y-shaped seal ring of the washing mechanism in the rock drill using finite element simulation analysis. These results can help evaluate how various structural parameters affect the Y-shaped water seal's ability to seal.

Equivalent stress

Higher equivalent or Von Mises stress levels generally make materials more prone to deterioration like relaxation and cracking, which eventually results in a shorter lifespan. The Y-shaped seal ring is most susceptible to seal failure at the top of its inner and outer lips as well as the lip valley, as shown in Fig. 5, where the greatest concentration of Von Mises stress occurs when the ring is subjected to rotary impact.

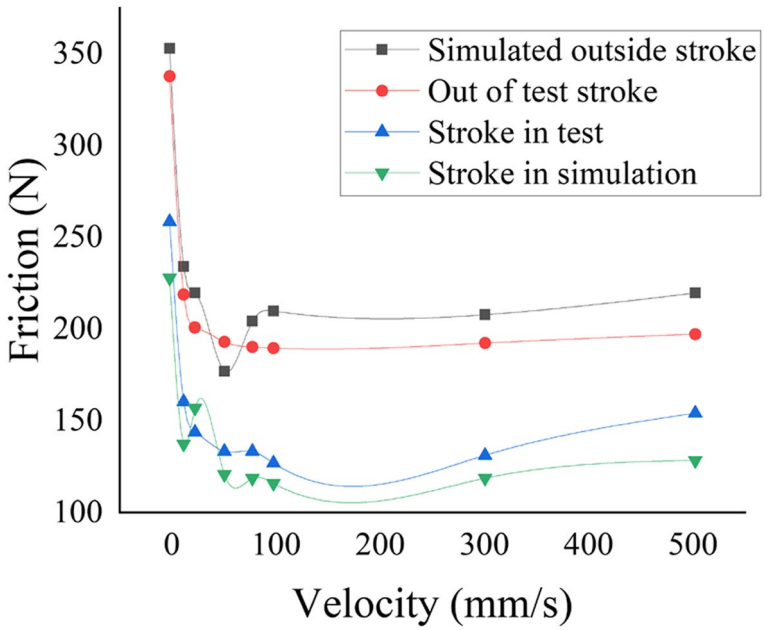

Fig. 4 Comparison of simulation and experiment results

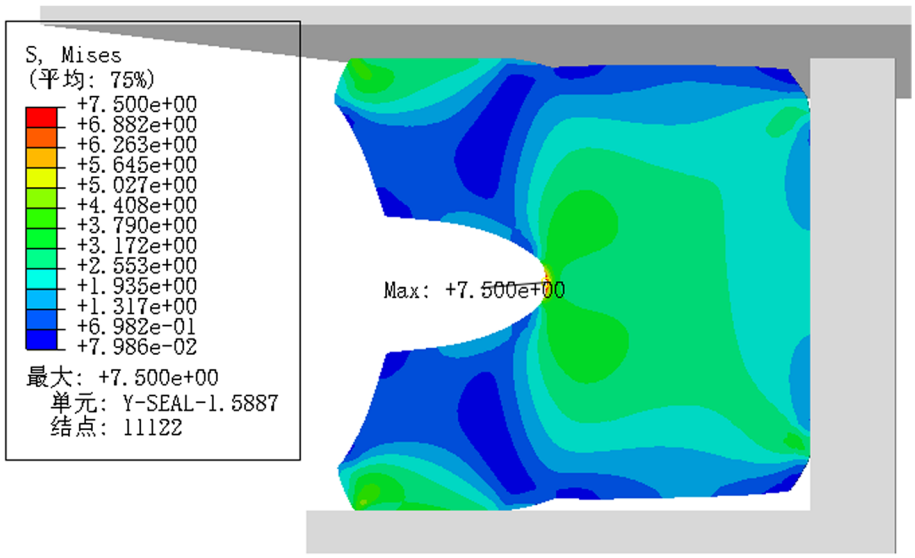

Fig. 5 Von Mises stress nephogram

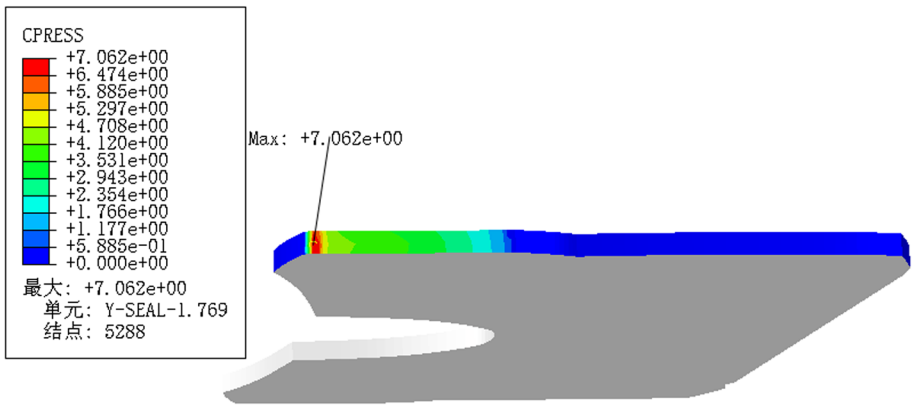

Fig. 6 Cloud diagram of contact stress

Contact stress

The sealing effectiveness of the seal ring is directly influenced by the contact stress. If the maximum contact stress surpasses the water pressure theoretically, it can provide a sealing effect for high-pressure flushing water. The higher the maximum contact stress, the better the sealing performance. However, excessively high contact stress will result in significant friction, quick wear, and damage to the seals. Since the water seal encounters complex motion and is affected by the inadequate lubrication provided by the water medium, the wear is intense, and the contact stress cannot be too high. As illustrated in Fig. 6, the contact stress of the water seal mainly focuses on the seal lip, and the highest contact stress is at the lip's apex.

The nephograms reveal that the lower the maximum Von Mises stress and the highest contact stress, the better the sealing ability. Therefore, the optimization and improvement of the sealing structure should focus on the structural parameters of the upper and lower sealing lip and the lip valley.

Simulation results analysis

Orthogonal testing is a powerful technique for studying complicated relationships between components, finding novel patterns, and reducing testing time. In this work, we utilized finite element modeling and orthogonal testing methodologies to explore the impact of geometric parameters on the sealing performance of Y-shaped seal ring sections.

Orthogonal experimental design

Based on the existing literature, the essential considerations in developing the orthogonal test for the Y-shaped seal ring are the structural characteristics linked to the seal lip and lip valley. Therefore, this research picks six significant structural factors to increase the ring's structure and reduce the maximum contact stress and maximum Von Mises stress. A six-factor, five-level orthogonal test is essential for the section geometric parameters, which include lip thickness (A), chamfer length (B), lip length (C), lip depth (D), the included angle of the lip valley (E), and the included angle of the lip and drill tail (F). The factor level table for the orthogonal test of section geometric parameters is presented in Table 1. The standard orthogonal table is applied for the orthogonal test.

Effect of Y-shaped water seal structure dimensions on sealing performance

It is presumed that each influencing element is autonomous and does not impact the others. The calculation results of the orthogonal design scheme entail summing and averaging the maximum contact stress and maximum Von Mises stress at each level of each component to create the connection curve between the goal parameters and other influencing variables. Figure 8 depicts the link between each contributing component and the maximal contact and Von Mises stresses. The original values of the geometrical parameters were lip thickness $A=2$ mm, chamfer length $B=0.47$ mm, lip length $C=2.3$ mm, lip depth $D=1.95$ mm, lip-valley angle $E=50°$, lip-braze-tail angle $F=25°$.

According to Fig. 7, the elements that substantially impact the maximum contact stress are lip thickness (A), chamfer length (B), and lip length (C). As shown in Fig. 7a, the maximum contact stress of the primary sealing surface rises generally with the increase in lip thickness (A), and when the lip thickness (A) is between 2.2 mm and 2.4 mm, its impact on the maximum contact stress of the primary sealing surface is modest. As shown in Fig. 7b, the maximum contact stress of the main sealing surface is roughly proportional to the chamfer length (B) and increases fast with the rise of chamfer length (B). When the chamfer length (B) is between 0.42 mm and 0.47 mm, the growth rate slows

Table 1 Orthogonal test factor level of section geometric parameters

Level	Factor					
	A/mm	*B*/mm	*C*/mm	*D*/mm	*E*/°	*F*/°
1	1.6	0.37	1.9	1.75	50°	17°
2	1.8	0.42	2.1	1.85	52°	19°
3	2	0.47	2.3	1.95	54°	21°
4	2.2	0.52	2.5	2.05	56°	23°
5	2.4	0.57	2.7	2.15	58°	25°

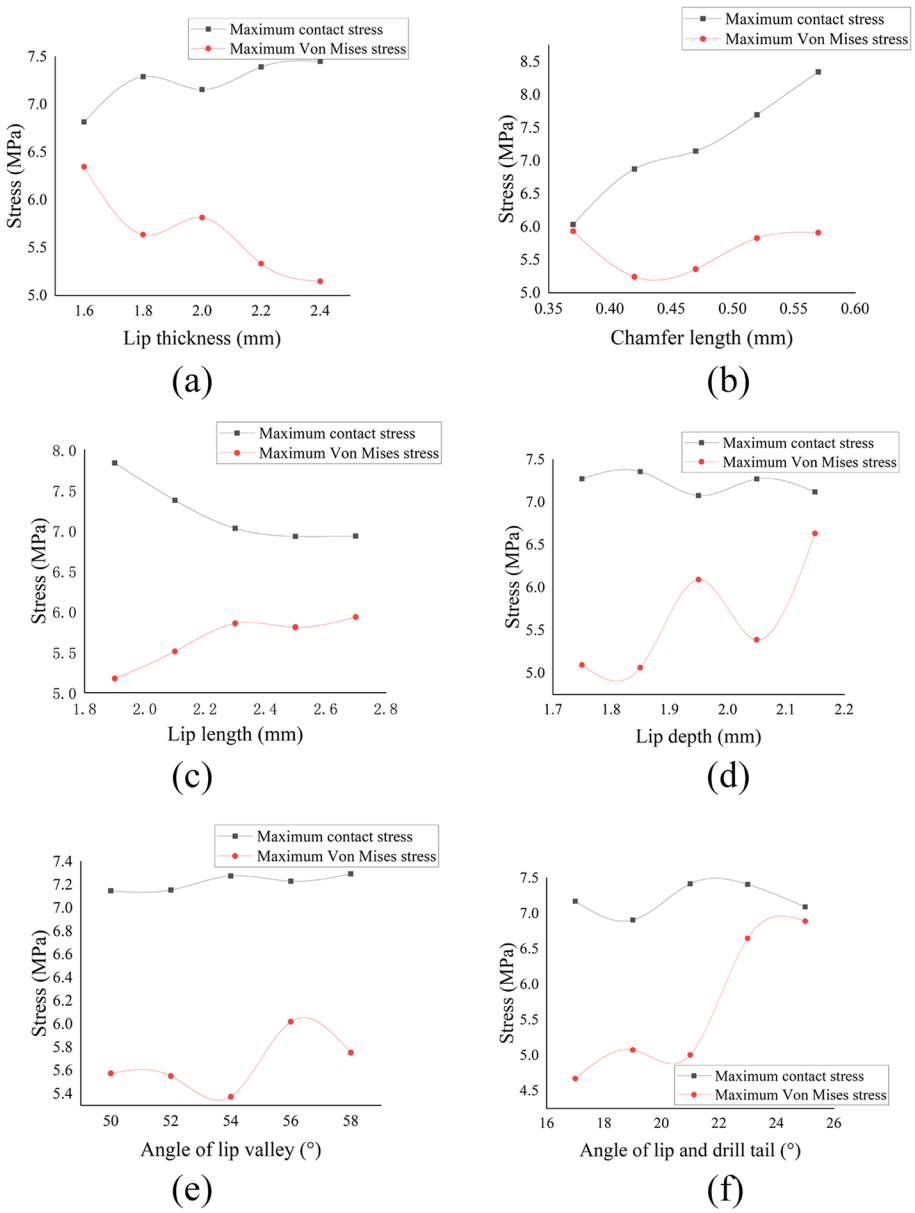

Fig. 7 Influence of structural parameters on the performance of Y-ring

down and then climbs quickly again. The reason why the maximum contact stress of the primary sealing surface rises with the increase in lip thickness (*A*) and chamfer length (*B*) is largely because the Y-shaped sealing ring seals mainly via the contact between the sealing lip and the tail. The increase in lip thickness (*A*) and chamfer length (*B*) enhances the stiffness of the sealing lip, resulting in larger contact stress and more visible stress concentration under the same preload. In contrast, raising the lip length (*C*) lowers the stiffness of the sealing lip and minimizes the contact stress.

The key elements that have a substantial influence on the maximum Von Mises stress are the lip thickness (*A*), the lip depth (*D*), and the included angle of the lip and drill tail (*F*). As demonstrated in Fig. 7a, raising the lip thickness (*A*) greatly decreases the

maximum Von Mises stress, resulting in a large reduction range. However, regarding the lip depth (*D*) and the included angle of the lip and drill tail (*F*), the maximum Von Mises stress rises as they develop, as seen in Fig. 7d, f. Specifically, when the lip depth (*D*) decreases between 1.95 mm and 2.05 mm, there is a localized drop in the maximum Von Mises stress. In the case of the included angle of the lip and drill tail (*F*), its influence on the maximum Von Mises stress is essentially minimal if its value is below 21°. However, if its value surpasses 21°, the maximum Von Mises stress approximately proportionately grows because the angle directly impacts the contact area between the sealing lip and the tailstock. As the angle rises, the contact area gets smaller, resulting in stress concentration that makes the sealing ring more prone to relaxation and cracking, which negatively influences the product's service life.

Results and discussion

In engineering practice, increasing the construction parameters of seal rings includes analyzing numerous components' effects on the contact stress and von Mises stress of the seal ring. It is necessary to identify the value of each element for optimum sealing performance. To rapidly acquire the test optimization results, range analysis may be done to find major and secondary variables, optimum levels, optimal combinations, and optimal collocation depending on each factor's range size. The range size indicates the factor's influence and is computed by subtracting the lowest test value from the highest test value of each factor's distinct levels.

Minimization of maximum contact stress

Table 2 presents the results of the range analysis, which aims to minimize the maximum contact stress. The factors affecting the maximum contact stress in descending order of magnitude are *B*, *C*, *A*, *F*, *D*, and *E*. This indicates that the chamfer length (*B*) has the most significant impact on the maximum contact stress of the main sealing surface, followed by the lip length (*C*) and lip thickness (*A*). The effects of the included angle of the lip and drill tail (*F*), lip depth (*D*), and the included angle of the lip valley (*E*) are marginal. The proposed plan for improvement is $A_1B_1C_4D_3E_1F_2$.

Minimization of peak Von Mises stress

The range analysis findings for reducing peak Von Mises stress are provided in Table 3. The contributing elements on maximum Von Mises stress are classified as *F*, *D*, *A*, *C*, *B*, and E in order of magnitude. This means that the included angle of the lip and drill

Table 2 Analysis results under the maximum contact stress objective

Project	*A*	*B*	*C*	*D*	*E*	*F*
k_1	6.817	6.037	7.838	7.275	7.148	7.173
k_2	7.291	6.877	7.376	7.358	7.156	6.908
k_3	7.156	7.148	7.029	7.079	7.277	7.419
k_4	7.393	7.698	6.929	7.273	7.231	7.411
k_5	7.451	8.347	6.935	7.121	7.295	7.093
Range	0.634	2.310	0.909	0.279	0.147	0.511

Table 3 Analysis results under the maximum von Mises stress objective

Project	*A*	*B*	*C*	*D*	*E*	*F*
k_1	6.348	5.936	5.176	5.096	5.576	4.671
k_2	5.636	5.243	5.511	5.065	5.553	5.076
k_3	5.816	5.360	5.853	6.092	5.375	5.006
k_4	5.333	5.830	5.808	5.392	6.021	6.650
k_5	5.148	5.911	5.931	6.635	5.755	6.893
Range	1.200	0.693	0.755	1.570	0.646	2.222

Table 4 Analysis of range proportion

Target parameters	*A*	*B*	*C*	*D*	*E*	*F*
Maximum contact stress	0.132	0.482	0.190	0.058	0.031	0.107
Maximum Von Mises stress	0.169	0.098	0.107	0.22	0.091	0.314
Average value	0.151	0.290	0.149	0.139	0.061	0.211

tail (F) has the largest influence on maximum Von Mises stress. Lip depth (*D*) and lip thickness (*A*) have a substantial impact, although the effects of lip length (*C*), chamfer length (B), and the included angle of the lip valley (*E*) are modest. The upgrade plan is $A_5B_2C_1D_2E_3F_1$.

Optimization results and analysis

Due to variances in goal criteria, the improvement plans for the two components reveal substantial disparities. To comprehensively assess the conclusion of the range analysis of each indicator, taking into consideration both goal parameters, the proportion of each factor's range in each indicator was calculated. The average percentage of the same element was next evaluated, as presented in Table 4. It is obvious that when considering both target parameters, the factor impact sequence is *B, F, A, C, D,* and *E.* This implies that the chamfer length (*B*) and the included angle of the lip and drill tail (F) have a significant influence on the sealing ring performance, followed by the lip thickness (*A*), lip length (*C*), and lip depth (*D*); the impact of the included angle of the lip valley (*E*) is relatively minor. The overall renovation plan is $A_5B_1C_4D_2E_3F_1$.

Based on the analysis results, a Y-shaped sealing structure has been designed via full evaluation of numerous aspects affecting contact stress and Von Mises stress. The size parameters are $A=2.4$ mm, $B=0.37$ mm, $C=2.5$ mm, $D=1.85$ mm, $E=54°$, and $F=17°$. To validate if these parameters are optimum, simulation analysis was done, and the findings are reported in Figs. 8 and 9. The findings suggest that the maximum contact stress and maximum Von Mises stress are 6.375 MPa and 4.127 MPa, respectively. A comparison of the results reveals that at the same water pressure and rotating speed, the maximum contact stress and maximum Von Mises stress for the Y-shaped seal ring decreased by 15% and 45%, respectively, significantly improving the ring's performance and increasing its service life due to the large decrease in maximum Von Mises stress. The study of the stress distribution of seals by means of simulation is a widely used and reliable means, however, in the process of utilizing simulation, the influence of many

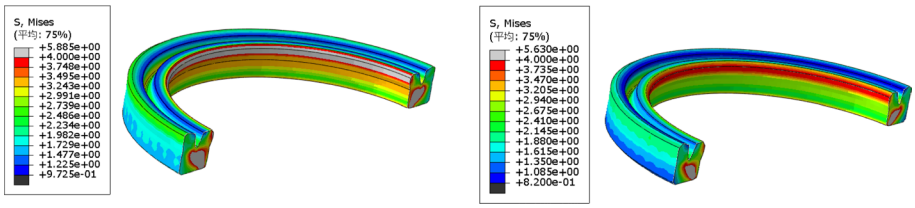

(a) Under original structural parameters (b) Orthogonal optimization scheme

Fig. 8 Equivalent stress comparison. **a** Under original structural parameters. **b** Orthogonal optimization scheme

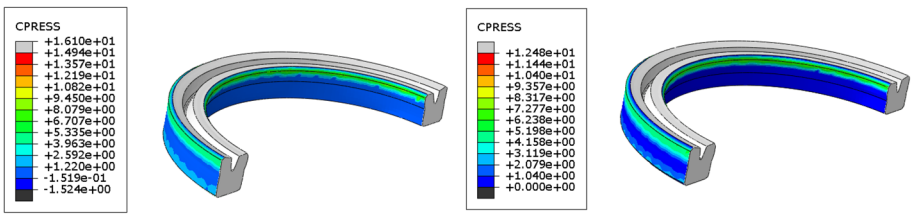

(a) Under original structural parameters (b) Orthogonal optimization scheme

Fig. 9 Contact stress comparison. **a** Under original structural parameters. **b** Orthogonal optimization scheme

secondary factors is neglected and errors are inevitable. The correctness of the research method and simulation model of this paper can be verified by subsequent experiments.

Conclusions

(1) Within the range of values examined by the orthogonal technique, the maximum contact stress of the objective parameter is significantly impacted by lip thickness (*A*), chamfer length (*B*), and lip length (*C*). Specifically, the maximum contact stress rises with an increase in lip thickness (*A*) and chamfer length (*B*), and reduces with an increase in lip length (*C*). The maximum Von Mises stress of the target parameter is greatly affected by the lip thickness (*A*), lip depth (*D*), and the included angle of the lip and drill tail (*F*). Specifically, the maximum Von Mises stress rises with an increase in lip depth (*D*) including the angle of the lip and drill tail (*F*), and reduces with an increase in lip thickness (*A*).

(2) Through the range ratio analysis, the effect of each structural parameter on the sealing performance is identified. The chamfer length and the included angle of the lip and drill tail have a stronger impact on the working performance of the seal ring, followed by the thickness, length, and depth of the lip. The included angle of the lip valley has the least impact. Through range ratio analysis, the influence of each structural parameter on sealing performance is found. The chamfer length (*B*) and the included angle of the lip and drill tail (*F*) have the most important influence on the seal ring's operating performance, followed by the lip's thickness (*A*), lip length (*C*), and lip depth (*D*). The included angle of the lip valley (*E*) has the least influence.

(3) An improved design has been provided for the Y-shaped sealing ring construction of the washing mechanism in the rock drill. When operating under similar circumstances, the Y-shaped seal ring demonstrates a 15% fall in maximum contact stress and a 45% reduction in maximum Von Mises stress. Consequently, the sealing performance is substantially improved.

Acknowledgements
Not applicable.

Authors' contributions
Conceptualization: CJ and LY. Methodology: CJ and LZ. Software: LZ. Validation: CJ and LZ. Formal analysis: LZ. Investigation: CJ. Resources: LY. Writing—original draft preparation: LZ. Writing—review and editing: CJ and AW. All authors have read and approved the final manuscript.

Funding
This project is funded by the Basic Scientific Research Project of Liaoning Province's Education Department in China (LJKMZ20220921).

Availability of data and materials
The data that supports the findings of this study are available within the article.

Declarations

Competing interests
The authors declare that they have no competing interests.

Received: 26 May 2023 Accepted: 24 December 2023
Published online: 08 January 2024

References

1. Lei Y, Chen K, Zhan C (2020) Optimization of structural parameters of Y-ring based on reciprocating motion of servo hydraulic cylinder. Metall Equip (04):1–5 + 33
2. Wang G, Hu G, He X, Dong S, Chen B (2014) Sealing performance analysis of Y-ring for reciprocating seal shaft. Mech Design Res 30(06):37–42+ 46
3. Bin Li, Da W, Chunlei Y (2019) Structural optimization design of flexible seal ring for flat gate valve of Christmas tree. Lubr Seal 44(11):105–111
4. Ming L, Jun J, Dong D (2012) Discussion on sealing principle and structural optimization design of Y-ring. Spec Rubber Prod 33(03):57–59
5. Liu H, Wang B, Meng X, Lu M, Peng X (2017) Structure optimization of high-pressure X-ring based on orthogonal test. Lubric Seal 42(07):106–110+ 134
6. Hanyu G, Li JD, Bin LL, Jiabin S, Qianjin Y (2019) Study on sealing performance of hydraulic slip ring spring energy storage seal in single point mooring system. Lubric Seal 44(12):75–80
7. Chengliang C, Hanyu G, Xinyu W, Gang W, Qianjin Y (2020) Finite element analysis of rubber seal ring performance of steel pile stopper for offshore wind turbine. Rubber Industry 67(04):287–293
8. Türköz M, Evcen DC (2022) Investigation on the sealing performance of polymers at ultra high pressures. Int Polym Proc 37(05):549–558
9. Dong K, Ni G, Xu Y (2021) Effect of optimized pore structure on sealing performance of drilling sealing materials in coal mine. Constr Build Mater 274(08):121765
10. Huarong M, Xuedong L, Boxian Li (2016) Stress analysis and structure optimization of Y-shaped rubber seal ring for autoclave. Lubr Seal 41(03):107–113
11. Zhou X, Yanhui Wu, Xin G (2022) Numerical study on sealing characteristics of high-pressure turbine cylindrical hole radial rim seal. Tuijin Jishu/J Propulsion Technol 43(02):161–170
12. Ai HT, Di LXT, Suo SF, Huang L (2015) Finite element analysis of reliability and sensitivity of Y-ring. Lubr Seal 40(05):5–10+ 15

Publisher's Note